Article

Interlayer Properties of In-Situ Oxidized Porous Stainless Steel for Preparation of Composite Pd Membranes

Laura Furones and David Alique *

Department of Chemical and Energy Technology, Chemical and Environmental Technology, Mechanical Technology and Analytical Chemistry, Rey Juan Carlos University, C/Tulipán s/n, 28933 Móstoles, Spain; laura.furonesm@gmail.com
*   Correspondence: david.alique@urjc.es; Tel.: +34-91-488-76-03; Fax: +34-91-488-70-68

Abstract: Hydrogen is considered as a real alternative for improving the current energy scenario in the near future and separation processes are a crucial step for the economy of the process in both centralized and distributed production systems. In this context, Pd-based composite membranes appear as an attractive technology trying to reduce the Pd thickness by modifying the commercial supports, mainly formed by metals to fit properly in conventional industrial devices. In most cases, a final calcination step is required and hence, the metallic support can be oxidized. This work analyzes in detail the properties of intermediate layers generated by in-situ oxidation of tubular PSS supports as a crucial step for the preparation of Pd/PSS membranes. The oxidation temperature determines the modification of original morphology and permeability by increasing the presence of mixed iron-chromium oxides as temperature rises. A compromise solution need to be adopted in order to reduce the average pore mouth size and the external roughness, while maintaining a high permeation capacity. Temperature of 600 °C lets to reduce the average pore size from 3.5 to 2.1 μm or from 4.5 to 2.3 μm in case of using PSS supports with 0.1 or 0.2 μm porous media grades, respectively but maintaining a hydrogen permeation beyond targets of United States of America Department of Energy (US DOE). Lower temperatures provoke an insufficient surface modification, while greater values derive in a drastic reduction of permeability. In these conditions, two composite membranes were prepared by ELP-PP, obtaining 14.7 and 18.0 μm thick palladium layers in case of modifying PSS tubes of 0.1 or 0.2 μm media grades, respectively. In both cases, the composite Pd membranes exhibited a hydrogen perm-selectivity greater than 2000 with permeances ranged from 2.83 to $5.84 \cdot 10^{-4}$ mol m^{-2} s^{-1} Pa$^{-0.5}$ and activation energies of around 13–14 kJ mol^{-1}.

Keywords: porous stainless steel; in-situ oxidation; surface modification; palladium membrane; hydrogen

1. Introduction

Hydrogen is considered as a real alternative to improve the energy scenario currently based on fossil fuels, promoting the use of renewable energies in the near future [1,2]. Ideally, water can be split with help of renewable energies to produce hydrogen, generating a very low environmental impact [3–5]. However, diverse studies affirm that a transition period will be need before this ideal situation become profitable, using a wide variety of raw materials for both centralized and distributed hydrogen production systems [6–10]. In this context, new routes from waste materials are being widely studied in the last years, considering both solid matter such as biomass [11], plastics [11], tea [12] or industrial municipal wastes [13] and liquids, in example olive mill wastewater [14]. In most of these cases, hydrogen purification is required for particular applications, i.e., combustion engines, turbines or fuel cell systems and Pd-based membranes are suggested as an attractive technology [15–17] to be used

as independent separator [18,19] or in a membrane reactor configuration [17,20]. These membranes are usually incorporated onto a substrate to reduce the film thickness and simultaneously maintain a suitable mechanical stability [21–23]. Only a few works propose the use of relatively thick unsupported films [24,25]. A wide variety of materials has been suggested for the preparation of supported Pd-based membranes, highlighting the porous metals [23,26] and the ceramic ones [18,27]. The properties of supports have a clear influence on the membrane performance, despite an ideal solution is not adopted. In general, ceramic supports with a smooth surface and narrow pore sizes provide a better surface for the membrane preparation [28–30] but the limited mechanical resistance and diverse thermal expansion coefficient to that of palladium jeopardize the membrane lifespan [18]. On the other hand, metallic supports present an exceptional mechanical resistance that ensures good sealing and suitable integration in conventional stainless steel devices [31,32], although the rougher surface with relatively large pore sizes hinders the preparation of a thin and free-defect Pd film [31,33]. The incorporation of an additional intermediate layer is one of the most popular alternatives to overcome these problems [34–36] and, additionally, it is able to prevent metal interdiffusion processes that could cause a drastic permeation drop when operating at high temperatures [37]. A wide variety of materials has been proposed to be used as intermediate layers, including silica [38,39], ceria [40–42], zirconia [22,33,43,44] and micron-sized nickel and alumina slurries [45], among others [37,46–49]. In most cases, the calcination of the composite system is required in order to obtain the final structure of these materials [40,43] and, consequently, partial oxidation of the support is also produced. Thus, the generation of metal oxides derived from the calcination step is frequent and its evaluation is very important. In fact, it is also suggested the use these metal oxides themselves as an effective intermediate layer [36,50,51]. Thus, Ma et al. [51] proposed and patented a controlled in-situ oxidation of porous stainless-steel supports (PSS) for fabricating Pd-based composite membranes. They affirmed that temperatures higher than 600 °C generated enough oxides to prevent the undesirable intermetallic diffusion and to act as an effective intermediate barrier. Following this pioneer work, Guazzone et al. [50] calcined PSS supports in stagnant air at 400–500 °C to generate an effective intermediate layer to prevent the diffusion of PSS elements to the palladium layer. Mateos-Pedrero et al. [36] also studied the direct oxidation of supports in air at temperatures in the range 600–800 °C with a heating ramp rate of 2 °C min^{-1}. They ensure that the thickness of this intermediate layer was not enough to facilitate the generation of a thin palladium layer in a comparable grade to other alternatives but its presence had a negative effect on the permeate flow rate. More recently, Iulianelli et al. [52] also oxidized tubular PSS supports prior to incorporate a PdAu thin film by electroless plating. In this case, the support was oxidized for 12 h at a relatively low temperature (500 °C) and additionally modified with pre-activated alumina particles.

Taking into account the importance of PSS support modification by calcination in air on multiple membrane preparation methods and the scarce publications addressing this topic in detail, the present work analyzes both morphology modification and permeation performance of commercial porous stainless steel supports with diverse media grade after calcination in air. The generation of a mixed iron-chromium oxides were produced after dwelling a high temperature for 12 h. The influence of the calcination temperature of tubular 316L PSS supports with two different porous media grades (0.1 μm and 0.2 μm) has been studied in detail, as well as the consequences for the latter in palladium incorporation when using the electroless pore-plating method. All results have been discussed in terms of achieving the DOE technical targets for Pd-based membranes, obtaining relevant information compared to the current state of the art.

2. Materials and Methods

2.1. Membrane Preparation

In this work, symmetric 316L porous stainless steel (PSS) supports were purchased from Mott Metallurgical Corp. (Farmington, CT, USA) with tubular geometry and diverse commercial media

grades (0.1 and 0.2 µm). Original tubes presented a total length of 60 cm and outer diameter of 1.29 mm, preparing smaller pieces with 30 mm in length for the entire range of experiments collected here.

The general procedure to prepare the composite PSS-Pd membranes involves four successive steps, as we already published in detail elsewhere [18,23,53,54]: (i) initial cleaning with a sequence of acidic, alkaline and alcohol solutions in ultrasonic; (ii) intermediate layer generation; (iii) activation of the modified support and (iv) final palladium incorporation. This work is mainly focused in the second step, based on the generation of the mixed iron-chromium oxides intermediate layer formed by in-situ oxidation of commercial raw supports in air. Temperatures ranged from 550 to 700 °C were studied with heating and cooling ramp rates of 1.8 °C min^{-1} and dwelling time of 12 h at desired temperature. After that, the activation of the modified PSS supports was carried out by direct reduction of diluted $PdCl_2$ with hydrazine (0.2 M) in ammonia solution (2 M). Finally, the palladium film was incorporated by Electroless Pore-Plating (ELP-PP) to prepare the H_2 perm-selective composite membranes. In the last step, both plating bath (formed by palladium, ammonium, EDTA and water) and hydrazine solution (with a concentration of 0.2 M) were fed from opposite sides of the modified supports in order to force the chemical reaction just into the pores or, at least, in the nearest areas. Finally, the membranes were rinsed with deionized water and dried overnight at 110 °C.

2.2. Membrane Characterization

The membrane characterization includes a detailed study of the surface after each step during the synthesis procedure described before, as well as the permeation properties achieved after each modification.

The morphology of the external surface was analyzed by Scanning Electron Microscopy (Philips XL30 ESEM) equipped with an Energy Dispersive Analytical System (EDAS) for microprobe analysis in order to determine elemental composition. The surface porosity was determined by two different techniques: SEM images segmentation with Digital Micrograph® software (external surface porosity) and mercury porosimetry (real bulk volumetric porosity). Additionally, the roughness of external surface at diverse stages has been also measured with an optical profiler equipped with a 5× focus lens (Zeta-20 Optical Profiler). Finally, the total amount of Fe-Cr mixed oxides generated by oxidation during the formation of the intermediate layer and palladium incorporated by ELP-PP were estimated by gravimetric analysis (electronic balance Kern & Sohn ABS-4 with a precision of 1.0×10^{-4} g).

Furthermore, the permeation behavior of fabricated membranes was also determined in a home-made permeator device described elsewhere [39,53]. In summary, each sample (raw material, modified support or final palladium composite membrane) was placed in a stainless-steel cell, ensuring the correct sealing with graphite O-rings. The feed stream was introduced in the inner side of the membrane, collecting the permeate flux on the external side without any carrier gas. Permeate was collected at ambient pressure, varying the retentate pressure in the range of 0.0–3.0 bar. Permeate fluxes were measured by a volumetric mass flow meter with a minimum detection limit of 1 mL h^{-1}.

3. Results and Discussion

3.1. Support Characterization

As we previously mentioned, commercial supports with two different media grades have been used in the present study: 0.1 and 0.2 µm. This parameter is directly related to the porosity of the material, indicating the particle size for guaranteeing a 95% of rejection by the filter. First, the surface of both samples has been characterized by SEM, collecting the images when using SE detection mode and 650× magnification in Figure 1. As it can be seen in both cases, the surface of the support is formed by 316L stainless steel particles with diverse sizes and geometries, obtaining a wide variety of external pores and a certain irregularity. This fact provokes a relative high surface roughness, R_a = 12.25 ± 2.0 µm, although certainly similar in diverse zones of the external surface. The elemental composition determined from EDAS microprobe analysis evidences values within the range of a typical

316L stainless steel material: 63–64 wt % Fe, 17 wt % Cr, 9 wt % Ni, 2 wt % Mo and 8–9 wt % other elements with a very low content in carbon (<0.03 wt %). No meaningful differences can be observed for samples fabricated with media grades of 0.1 μm and 0.2 μm.
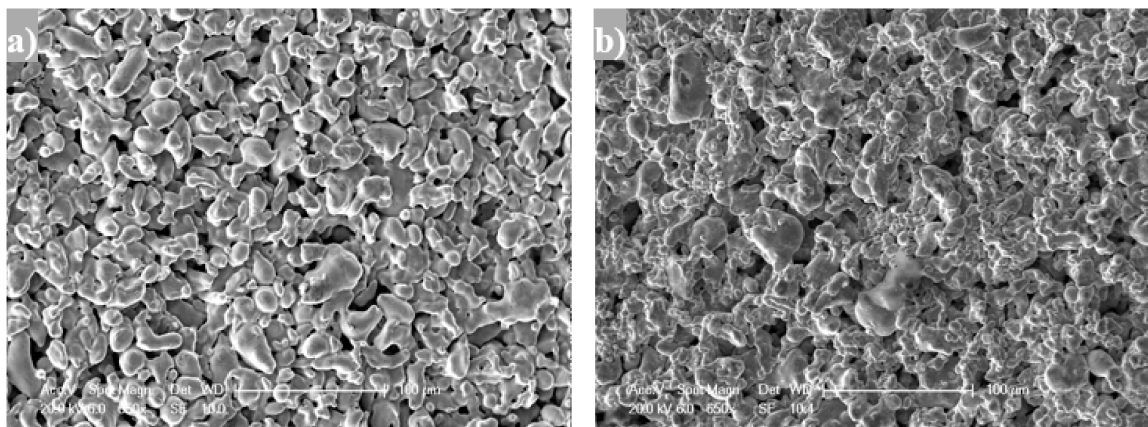
Figure 1. SEM images of PSS supports with diverse commercial media grades: (**a**) 0.1 μm and (**b**) 0.2 μm.

On the other hand, the pore size distribution determined by SEM image segmentation (Figure 2) indicates noticeable differences between both media grades, in spite of obtaining similar average porosities of around 20% (accordingly to the certified value by the manufacturer). PSS support with a media grade of 0.1 μm presents around 80% of external pores within 0–4 μm (average pore diameter 3.5 μm) and maximum pore sizes up to 24 μm. These values increase in case of analyzing the support with a media grade of 0.2 μm, obtaining a wider range between 0 and 6 μm (average pore diameter 4.5 μm) and greater maximum pore sizes, up to 38 μm. Although the average pore size and the media grade are different parameters, it should be noted that in both cases the first one is greater than the specified media grade in more than one magnitude order. Moreover, in spite of PSS supports included in this manuscript are symmetric in radial direction, it could be possible that average pore-mouth in the surface will be significantly greater than bottle-neck in the bulk substrate. In order to determine possible differences between the external surface pore distribution determined by SEM image segmentation and the real volumetric pore size distribution in the bulk material, Figure 3 displays the results obtained after characterization by mercury porosimetry. This technique reveals average pore sizes diameters of around 1.9 and 2.8 μm for PSS supports of grade 0.1 and 0.2 μm, respectively. These values, in spite of being smaller than the previous ones, determined by image segmentation, are still larger than values certified by the manufacturer through the media grade parameter. This fact is a critical issue for the membrane preparation due to the minimum palladium thickness required to obtain a free-defect top coating being proportional to the maximum pore size of the support, as Mardilovich affirms in a previous manuscript [55].

Finally, the permeation capacity of the supports for nitrogen and hydrogen pure gases has been also determined and adopted as reference value for evaluating later modifications. Due to the smaller kinetic diameter of hydrogen respect to nitrogen molecule, a greater permeation of the first gas has been achieved in all cases with an ideal perm-selectivity (determined as the ratio of individual hydrogen and nitrogen permeate fluxes [56]) around 2.5. Analyzing in detail the results obtained for each commercial PSS media grade, almost double permeation capacity can be achieved when using a media grade of 0.2 μm instead of 0.1 μm, obtaining hydrogen permeate fluxes of 3.61 and 1.78 mol m^{-2} s^{-1}, respectively (measured at T = 400 °C and ΔP = 1.0 bar).
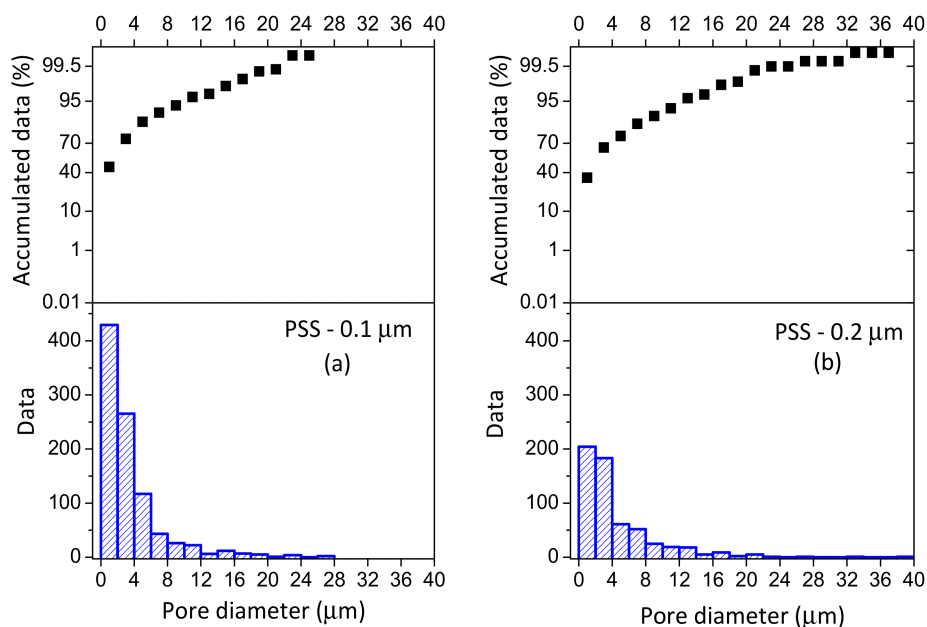
Figure 2. Pore size distribution by SEM image segmentation of PSS supports with diverse commercial media grades: (**a**) 0.1 μm and (**b**) 0.2 μm.
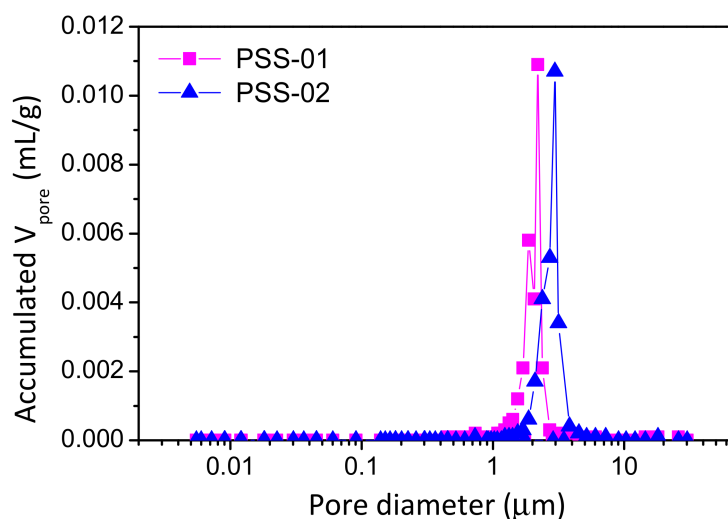
Figure 3. Pore size distribution by mercury porosimetry of PSS supports with diverse commercial grades: 0.1 μm and 0.2 μm.

3.2. Intermediate Layer Formation by In-Situ Oxidation

As it is previously determined, commercial PSS supports are formed basically by iron, chromium nickel and molybdenum, being prevalent the first two elements. Both iron and chromium are susceptible to be oxidized in a major grade due to their standard reduction potential values ($E^0 \times (Cr^{3+}/Cr^0) = -0.740$ V, $E^0 \times (Fe^{2+}/Fe^0) = -0.440$ V, $E^0 \times (Ni^{2+}/Ni^0) = -0.250$ V and $E^0 \times (Mo^{3+}/Mo^0) = -0.200$ V). In this manner, the oxides formed by direct calcination of PSS supports in air atmosphere will derive mainly in a mixture of iron and chromium oxides. Both oxides have a Tamman temperature of 780 and 1081 °C, respectively, so they are good candidates to be used as an effective intermediate layer for preventing the metal diffusion of iron (Tamman temperature around 550–560 °C) and palladium (Tamman temperature of 640 °C), which is usually derived in a fatal damage of membranes when operating at high temperatures for long times [57].

Figure 4 shows the SEM images obtained after in-situ oxidation of PSS supports at diverse conditions, mainly varying the temperature of the treatment. No significant differences respect to the original substrates (see micrographs in previous Figure 1) have been obtained for mild conditions (T = 550 °C), independently of considering media grade of 0.1 or 0.2 μm. However, it is possible to appreciate a certain surface modification as the temperature of the process increases (upper than 600 °C) by the generation of oxide particles, decreasing the average pore size and appearing a slight additional roughness around each steel particle of the support. This effect is drastic in case of using the highest oxidation temperature (T = 700 °C), losing most of the original porosity of the support. This behavior seems to be certainly similar in case of using supports with media grade of 0.1 or 0.2 μm.
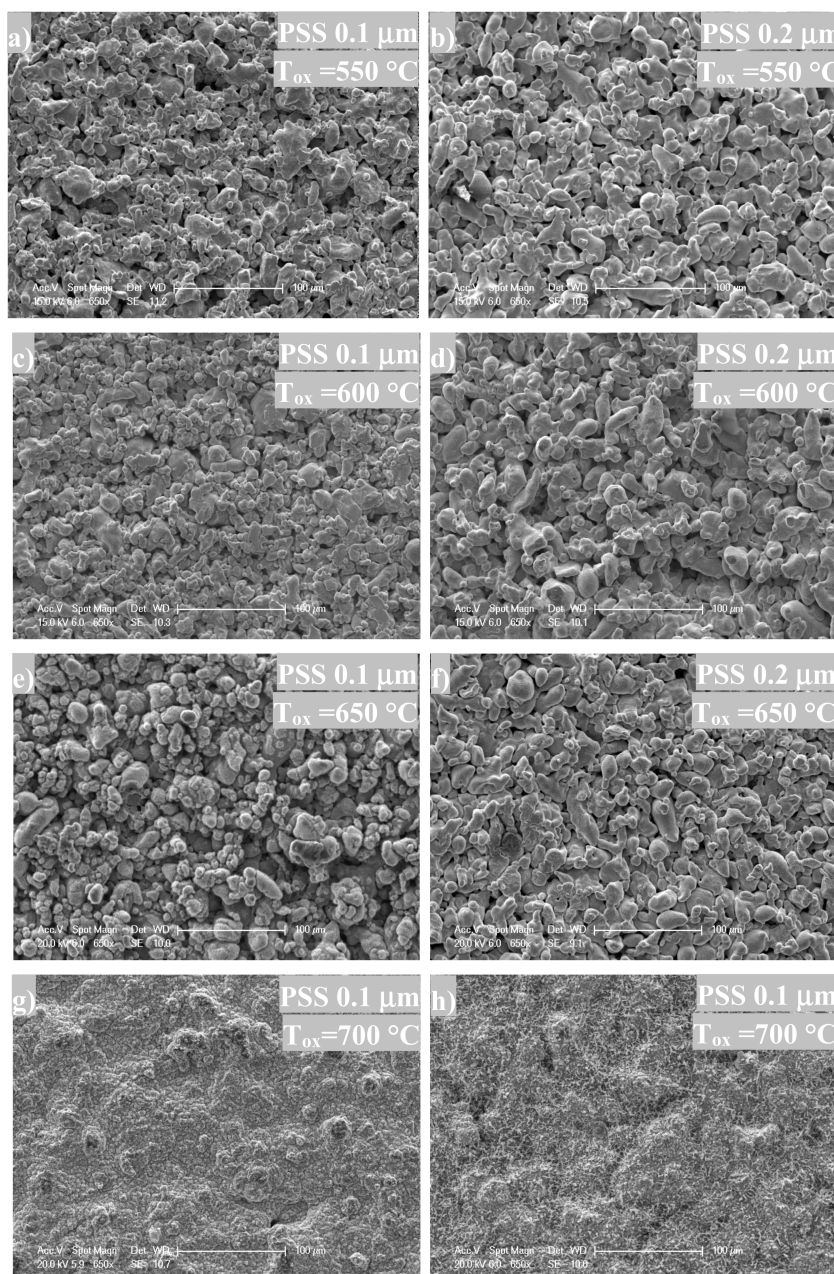
Figure 4. SEM images of PSS supports after 12 h in-situ oxidation: (**a**) media grade 0.1 μm, T_{ox} = 550 °C; (**b**) media grade 0.2 μm, T_{ox} = 550 °C; (**c**) media grade 0.1 μm, T_{ox} = 600 °C; (**d**) media grade 0.2 μm, T_{ox} = 600 °C; (**e**) media grade 0.1 μm, T_{ox} = 650 °C; (**f**) media grade 0.2 μm, T_{ox} = 650 °C; (**g**) media grade 0.1 μm, T_{ox} = 700 °C; and (**h**) grade 0.2 μm, T_{ox} = 700 °C.

With the aim of analyzing exhaustively the effect of temperature in the formation of Fe-Cr oxides and, consequently, the modification of the original PSS supports, Table 1 collects some important parameters, such as weight variation (Δm/L), external porosity (ε), surface average pore diameter (d_p), surface roughness (R_a) and EDAS analysis. A clear relationship between temperature of the treatment and formation of oxides species can be observed, increasing both weight gain and presence of oxygen as the temperature rises. The generation of these oxides derived in a slight reduction of the external roughness, mainly due to different elevation of PSS particles on the surface but a pronounced decrease in both average pore diameter and porosity. In fact, in case of using the highest temperature (T = 700 °C), only some residual porosity around 1.5% can be detected in the external surface. In general, similar values were achieved independently of the media grade considered. Here, it is important to emphasize the evolution of surface composition with the temperature of the oxidation process. The general trend shows a continuous increase in oxygen content, while both iron and chromium decreases due to the increasing generation of oxides as temperature rises. However, it is important to take into account that variation of chromium content depends on both media grade of the support and temperature of the treatment. In fact, the chromium content, determined by EDAS analysis, varies in a major grade for the complete set of experiments when using supports with a media grade of 0.1 μm (from 17.0 wt % of the raw material to 10.6 wt % after treatment at 650 °C) instead of considering a media grade of 0.2 μm (from 16.9 wt % of the raw material to 14.2 wt % after treatment at 650 °C). A particular effect has been obtained for the highest temperature of the in-situ oxidation process, carried out at 700 °C, in which the chromium content decreases up to approximately 1.5 wt %, independently of the support grade. This behavior can be derived from the greater content in iron of PSS supports and the preferential oxidation of chromium, emphasized at severe temperatures of the oxidation process. At these conditions, iron atoms can migrate to the external surface, hiding the chromium ones with very stable oxides. Similar effects have been described by Ma et al. [51], indicating an almost constant ratio between iron and chromium content for moderate temperatures of calcination treatment with air but iron enrichment in case of increasing temperatures. In this work, an important effect of the media grade considered for PSS supports is also evidenced, obtaining a greater variation in chromium when a media grade of 0.1 μm has been studied.

Table 1. Modification after in-situ oxidation of PSS supports with diverse commercial grades.

Sample	Media Grade (μm)	T_{ox} (°C)	Δm/L (g/m)	ε (%)	d_p (μm)	R_a (μm)	Elemental Composition EDAS (wt %)		
							Fe	Cr	O
PSS-01	0.1	-	-	21.5	3.5	11.8	63.3	17.0	0.0
PSS-01-550	0.1	550	1.5	15.7	3.1	9.4	61.2	16.1	7.5
PSS-01-600	0.1	600	5.8	7.3	2.1	9.0	61.0	13.5	11.4
PSS-01-650	0.1	650	7.4	5.7	1.7	8.9	59.2	10.6	19.9
PSS-01-700	0.1	700	19.2	1.4	0.6	6.5	75.5	1.2	23.3
PSS-02	0.2	-	-	19.6	4.5	12.7	63.9	16.9	0.0
PSS-02-550	0.2	550	2.0	15.4	3.4	9.9	61.9	16.3	7.4
PSS-02-600	0.2	600	4.4	10.6	2.3	9.2	57.6	13.3	16.1
PSS-02-650	0.2	650	6.6	6.3	2.1	8.7	56.3	14.2	17.8
PSS-02-700	0.2	700	15.5	1.6	0.8	6.2	77.2	1.5	21.3

In order to complete the characterization of the modified supports, permeation experiments with pure nitrogen and hydrogen at 400 °C and pressure differences ranged from 0.5 to 1.0 bar were carried out (Table 2). In general, an increase of the oxidation temperature provokes a decrease in the permeation capacity of the support. This drop is critical in case of using an oxidation temperature of 700 °C, obtaining negligible permeate fluxes. This fact can be directly related with the modification of original porosity by the generation of mixed iron-chromium oxides. This drop in permeability is greater in the case of using PSS supports with 0.1 μm media grade due to the narrower initial pore

sizes with respect to the supports with a media grade of 0.2 µm. Of course, hydrogen permeation is always maintained higher than nitrogen permeation at similar conditions due to differences in kinetic diameters for both molecules. It is also important to note that no noticeable changes in the ideal perm-selectivity arise (always around 2.5–3.0), in spite of mentioned differences in permeability. At this point, it is crucial to determine the optimal conditions for the in-situ oxidation treatment in order to ensure an effective intermediate layer for both surface modification and intermetallic diffusion prevention, while a suitable permeation capacity is ensured. In this context, the US Department of Energy (US DOE) [58] proposed some tentative values for 2015. In this document, a minimum permeation capacity of 1.13 mol m^{-2} s^{-1} (T = 400 °C and ΔP = 6.4 bar) is stablished as technical target for introducing dense metallic membranes in the industrial processes for hydrogen production. In this manner, assuming that hydrogen permeation in Pd-based membranes usually follows the Sieverts' law, a minimum permeation flux of 0.43 mol m^{-2} s^{-1} is required for the membranes presented in this work at tested operating conditions (400 °C and 1 bar). Thus, only treatments carried out at temperatures up to 600 °C are suitable to obtain supports that accomplish this permeation target suggested by the US DOE, due to porous support need to overcome these values in order to get a final permeance of the composite Pd membrane achieving this target. Considering both modification of the external surface and permeation properties, 600 °C has been selected as the most appropriate temperature for in-situ oxidation of PSS supports.

Table 2. Permeation properties of modified PSS supports after in-situ oxidation.

Sample	Media Grade (µm)	T_{ox} (°C)	ΔP (bar)	J_{N_2} (mol m^{-2} s^{-1})	J_{H_2} (mol m^{-2} s^{-1})	α_{H_2/N_2}
PSS-01	0.1	-	0.5	0.30	0.79	2.7
			1.0	0.72	1.78	2.5
PSS-01-550	0.1	550	0.5	0.21	0.59	2.9
			1.0	0.49	1.37	2.8
PSS-01-600	0.1	600	0.5	0.12	0.31	2.7
			1.0	0.27	0.73	2.7
PSS-01-650	0.1	650	0.5	0.09	0.25	2.7
			1.0	0.21	0.57	2.7
PSS-01-700	0.1	700	0.5	-	-	-
			1.0	-	-	-
PSS-02	0.2	-	0.5	0.63	1.52	2.4
			1.0	1.48	3.61	2.4
PSS-02-550	0.2	550	0.5	0.48	1.16	2.4
			1.0	1.16	2.90	2.5
PSS-02-600	0.2	600	0.5	0.33	1.02	3.1
			1.0	0.82	2.36	2.9
PSS-02-650	0.2	650	0.5	0.20	0.60	3.0
			1.0	0.48	1.34	2.8
PSS-01-700	0.2	700	0.5	<1.02×10^{-5}	<1.02×10^{-5}	-
			1.0	<1.02×10^{-5}	<1.02×10^{-5}	-

3.3. Palladium Composite Membrane Preparation

The modified supports achieved by in-situ oxidation in air atmosphere at 600 °C for 12 h, conditions selected from previous experiments, were used to prepare composite Pd/PSS membranes for hydrogen separation applications. A thin palladium film was incorporated by ELP-PP technique, basically based on chemical reduction of amino-palladium complexes with hydrazine when both solutions are fed from opposite sides of supports, as it is described by the following chemical reaction:

$$2\,Pd(NH_3)_4^{2+} + N_2H_4 + 4\,OH^- \rightarrow 2\,Pd^0 + 8\,NH_3 + \uparrow N_2 + 4\,H_2O \qquad (1)$$
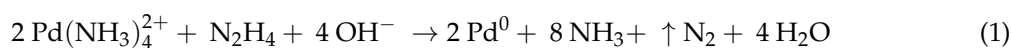
More details about this technique, including details of bath composition, temperature and duration of the process, can be consulted in our previous publications [18,20,53,54].

The final morphology of membranes prepared accordingly to this procedure when using in-situ oxidized PSS supports with diverse commercial media grades (0.1 and 0.2 μm) is shown in Figure 5. Here, both external surface and cross-section images are collected for each case. As it can be seen, independently of the commercial media grade, an apparent continuous layer of palladium was formed onto the modified supports. This fact, thoroughly discussed in our previous manuscripts [18,53], is mainly caused by the wide variety of pore sizes in the PSS supports, in spite of being modified by in-situ oxidation at high temperature for the generation of a Fe-Cr mixed oxides intermediate layer. In fact, the intermediate layer is really thin (only a few nanometers) and it cannot be easily determined by cross-sectional SEM images. On the other hand, the external Pd layer is certainly homogeneous and continuous, reducing the external porosity up to residual values ($\varepsilon = 0.0\%$ and $\varepsilon = 0.3\%$ for supports with media grades 0.1 and 0.2 μm, respectively). Also, the external roughness was smoothed after the incorporation of the Pd film, obtaining values around $R_a = 6.1 \pm 0.5$ μm in both cases. However, some differences can be appreciated for each particular case, specially attending to the film thickness. In this manner, the use of a modified PSS support with a media grade of 0.1 μm leads to obtain an average Pd thickness of 14.7 μm (average value from gravimetric analysis), while the use of a greater media grade for the modified PSS support provokes an increase of the Pd thickness up to 18 μm (also estimated from gravimetric measurements). In this manner, it can be affirmed that it is possible to obtain thinner Pd/PSS composite membranes when using a minor media grade in the PSS support. In this case, the benefits of smaller original pores and greater effects of modification by in-situ oxidation derived on the present values.
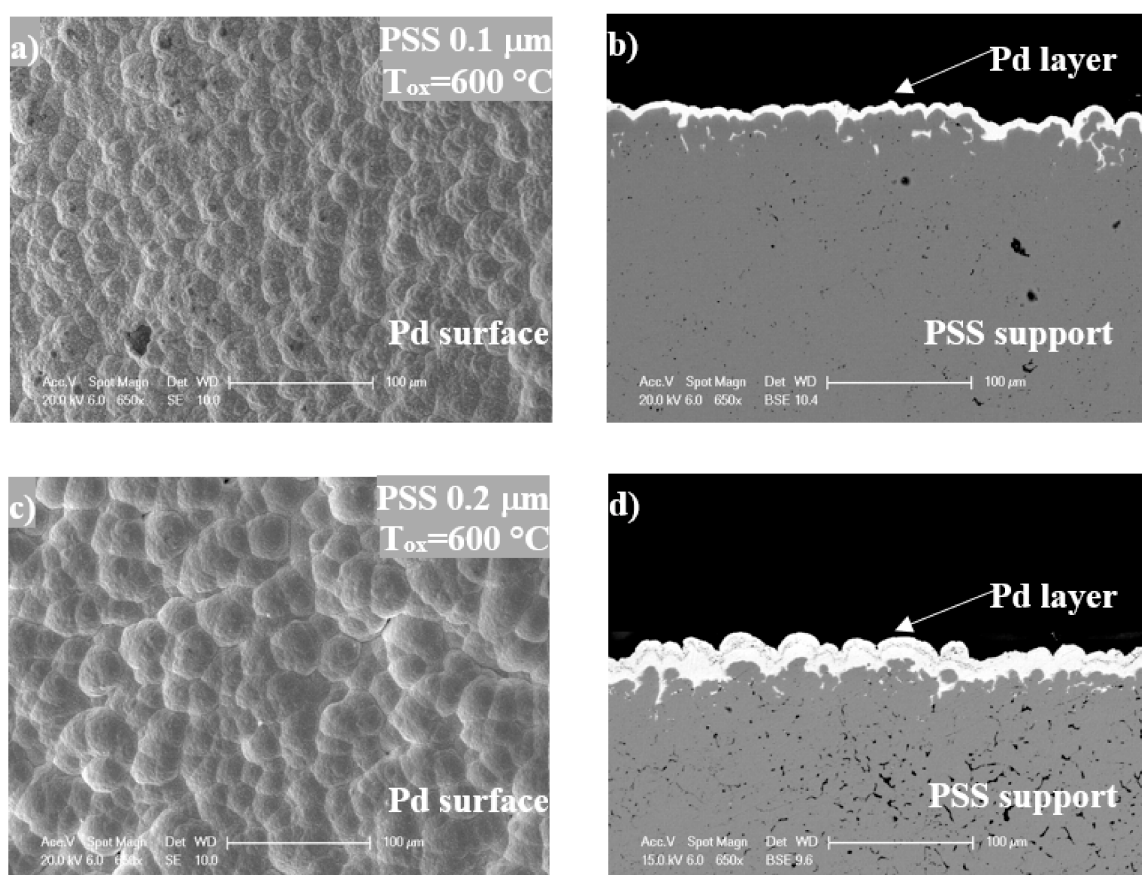
Figure 5. SEM images of modified supports (in-situ oxidation at 600 °C for 12 h) after Pd incorporation by ELP-PP: (**a**) media grade 0.1 μm, external surface; (**b**) media grade 0.1 μm, cross-section; (**c**) media grade 0.2 μm, external surface; and (**d**) media grade 0.2 μm, cross-section.

Finally, the permeation behavior of these membranes has been also evaluated and presented in Figure 6. Herein, it is important to emphasize that no nitrogen has been detected in the permeate side. Thus, considering the minimum detection limit of the volumetric mass flow meter (1 mL h^{-1}), a hydrogen perm-selectivity greater than 2000 is guaranteed. Moreover, analyzing the hydrogen permeation fluxes in detail, it can be mentioned that both membranes fulfill quite well the requirements of the Sieverts' law for all operating conditions, obtaining permeances in the range 4.01–5.84 $\times$ 10^{-4} mol m^{-2} s^{-1} Pa$^{-0.5}$ and 2.83–4.04 $\times$ 10^{-4} mol m^{-2} s^{-1} Pa$^{-0.5}$ for membranes Pd/PSS-01 and Pd/PSS-02, respectively. However, these values are lower than the proposed ones by the US DOE, in spite of this value has been not limited by the support modification, as we previously discussed. The diverse permeation capacity of both membranes is mainly caused by differences in the thickness of the palladium layer, which in turn is derived from the variance of surface properties, as we previously discussed. However, similar activation energies of around 13–14 kJ mol^{-1} are obtained in both cases, within the range of other published works.
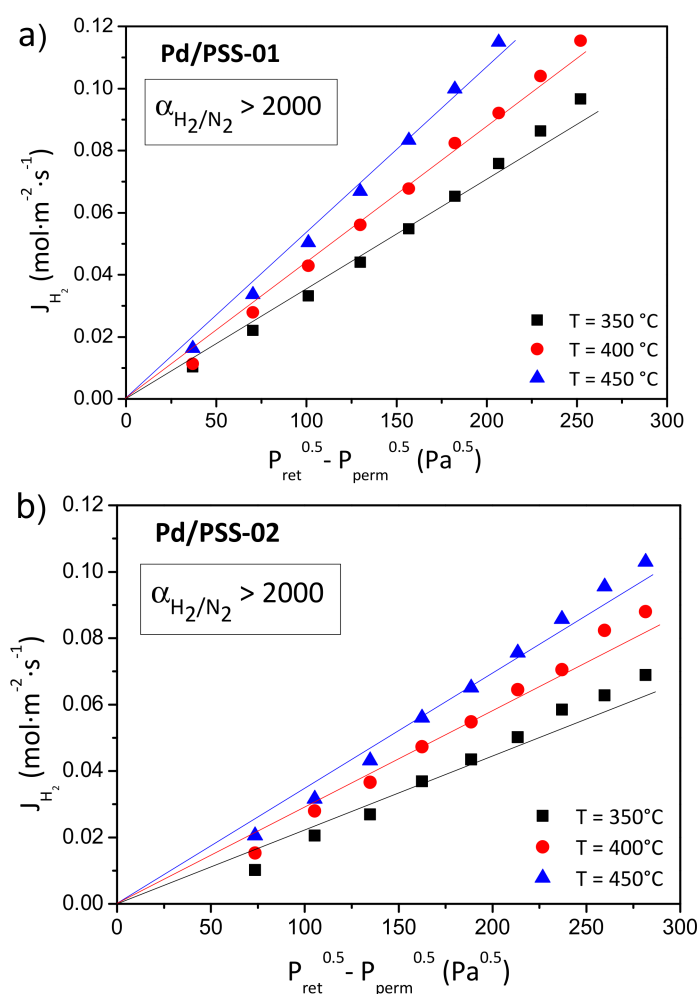
Figure 6. Permeation behavior of Pd-composite membranes prepared by ELP-PP over modified PSS supports with media grade 0.1 μm (**a**) and 0.2 μm (**b**).

4. Conclusions

The properties of intermediate layers generated by in-situ oxidation of tubular 316L PSS supports with two different commercial media grades have been studied as crucial parameters for the preparation of composite Pd membranes. The temperature of the oxidation treatment determines the achieved modification of the original morphology and permeability. Thus, the presence of mixed

iron-chromium oxides increases as the temperature rises, independently of media grade considered in the PSS support. Low temperatures do not modify in an important grade the original surface of supports, while the highest ones generate too many oxides that close most of the original porosity, decreasing drastically the permeation capacity of the modified supports. Moreover, it has been observed that the elemental composition of modified supports varies in a different way in case of varying the temperature and using diverse media grades for the porous supports. The preferential oxidation of chromium provokes an iron enrichment in case of increasing temperatures, emphasizing this effect when using a PSS support with a media grade of 0.1 μm. In this manner, a compromise solution need to be adopted in order to reduce both average pore mouth size and external roughness but simultaneously maintaining high porosity and hence, permeation capacity to avoid limitation of getting US DOE technical targets before incorporating the hydrogen selective layer. According to the results obtained, the oxidation process at 600 °C accomplished all these requirements: (i) the average pore size is reduced from 3.5 to 2.1 μm or from 4.5 to 2.3 μm in case of using PSS with commercial media grades 0.1 or 0.2 μm, respectively; (ii) but simultaneously, the hydrogen permeation flux stablished by US DOE targets for Pd composite membranes is not limited by the modified support. Taking into account these results, two composite membranes were prepared by ELP-PP, obtaining 14.7 and 18.0 μm thick palladium layers in case of using modified supports with 0.1 and 0.2 μm media grades, respectively. In both cases the membranes exhibited a hydrogen perm-selectivity greater than 2000 with permeances ranged from 2.83 to $5.84 \cdot 10^{-4}$ mol m^{-2} s^{-1} Pa$^{-0.5}$, lower than the values demanded by the US DOE technical targets. The activation energy in both cases was maintained around 13–14 kJ mol^{-1}.

Author Contributions: L. Furones and D. Alique conceived and designed the experiments; L. Furones performed the experiments; L. Furones and D. Alique analyzed the data; L. Furones and D. Alique contributed reagents/materials/analysis tools; D. Alique wrote the paper.

Conflicts of Interest: The authors declare no conflict of interest

References

1. Hanley; E.S.; Deane; J.P.; Gallachóir; B.P.Ó. The role of hydrogen in low carbon energy futures—A review of existing perspectives. *Renew. Sustain. Energy Rev.* **2017**. [CrossRef]
2. Vivas, F.J.; de las Heras, A.; Segura, F.; Andújar, J.M. A review of energy management strategies for renewable hybrid energy systems with hydrogen backup. *Renew. Sustain. Energy Rev.* **2018**, *82*, 126–155. [CrossRef]
3. Abbasi, T.; Abbasi, S.A. "Renewable" hydrogen: Prospects and challenges. *Renew. Sustain. Energy Rev.* **2011**, *15*, 3034–3040. [CrossRef]
4. Uyar, T.S.; Beşikci, D. Integration of hydrogen energy systems into renewable energy systems for better design of 100% renewable energy communities. *Int. J. Hydrog. Energy* **2017**, *42*, 2453–2456. [CrossRef]
5. Valente, A.; Iribarren, D.; Dufour, J. Harmonised life-cycle global warming impact of renewable hydrogen. *J. Clean. Prod.* **2017**, *149*, 762–772. [CrossRef]
6. García-García, F.R.; Soria, M.A.; Mateos-Pedrero, C.; Guerrero-Ruiz, A.; Rodríguez-Ramos, I.; Li, K. Dry reforming of methane using Pd-based membrane reactors fabricated from different substrates. *J. Memb. Sci.* **2013**, *435*, 218–225. [CrossRef]
7. Kim, C.-H.; Han, J.-Y.; Lim, H.; Lee, K.-Y.; Ryi, S.-K. Methane steam reforming using a membrane reactor equipped with a Pd-based composite membrane for effective hydrogen production. *Int. J. Hydrog. Energy.* **2017**. [CrossRef]
8. Kumar, B.; Kumar, S.; Kumar, S. Thermodynamic and energy analysis of renewable butanol–ethanol fuel reforming for the production of hydrogen. *J. Environ. Chem. Eng.* **2017**, *5*, 5876–5890. [CrossRef]
9. Tian, T.; Li, Q.; He, R.; Tan, Z.; Zhang, Y. Effects of biochemical composition on hydrogen production by biomass gasification. *Int. J. Hydrog. Energy* **2017**, *42*, 19723–19732. [CrossRef]

10. Tamošiūnas, A.; Valatkevičius, P.; Gimžauskaitė, D.; Valinčius, V.; Jeguirim, M. Glycerol steam reforming for hydrogen and synthesis gas production. *Int. J. Hydrog. Energy* **2017**, *42*, 12896–12904. [CrossRef]

11. Devasahayam, S.; Strezov, V. Thermal Decomposition of Magnesium Carbonate with Biomass and Plastic Wastes for Simultaneous Production of Hydrogen and Carbon Avoidance. *J. Clean. Prod.* **2017**, *174*, 1089–1095. [CrossRef]

12. Ayas, N.; Esen, T. Hydrogen production from tea waste. *Int. J. Hydrog. Energy.* **2016**, *41*, 8067–8072. [CrossRef]

13. Zahedi, S.; Solera, R.; García-Morales, J.L.; Sales, D. Effect of the addition of glycerol on hydrogen production from industrial municipal solid waste. *Fuel* **2016**, *180*, 343–347. [CrossRef]

14. Tosti, S.; Cavezza, C.; Fabbricino, M.; Pontoni, L.; Palma, V.; Ruocco, C. Production of hydrogen in a Pd-membrane reactor via catalytic reforming of olive mill wastewater. *Chem. Eng. J.* **2015**, *275*, 366–373. [CrossRef]

15. Li, H.; Caravella, A.; Xu, H.Y. Recent progress in Pd-based composite membranes. *J. Mater. Chem. A.* **2016**, *4*, 14069–14094. [CrossRef]

16. Rahimpour, M.R.; Samimi, F.; Babapoor, A.; Tohidian, T.; Mohebi, S. Palladium membranes applications in reaction systems for hydrogen separation and purification: A review. *Chem. Eng. Process. Process Intensif.* **2017**, *121*, 24–49. [CrossRef]

17. Arratibel Plazaola, A.; Pacheco Tanaka, D.; van Sint Annaland, M.; Gallucci, F. Recent Advances in Pd-Based Membranes for Membrane Reactors. *Molecules* **2017**, *22*, 51. [CrossRef] [PubMed]

18. Alique, D.; Imperatore, M.; Sanz, R.; Calles, J.A.; Giacinti Baschetti, M. Hydrogen permeation in composite Pd-membranes prepared by conventional electroless plating and electroless pore-plating alternatives over ceramic and metallic supports. *Int. J. Hydrog. Energy* **2016**, *41*, 19430–19438. [CrossRef]

19. Li, X.; Li, A.; Lim, C.J.; Grace, J.R. Hydrogen permeation through Pd-based composite membranes: Effects of porous substrate, diffusion barrier and sweep gas. *J. Memb. Sci.* **2016**, *499*, 143–155. [CrossRef]

20. Sanz, R.; Calles, J.A.; Alique, D.; Furones, L. H_2 production via water gas shift in a composite Pd membrane reactor prepared by the pore-plating method. *Int. J. Hydrog. Energy* **2014**, *39*, 4739–4748. [CrossRef]

21. Peters, T.A.; Stange, M.; Bredesen, R. On the high pressure performance of thin supported Pd–23%Ag membranes—Evidence of ultrahigh hydrogen flux after air treatment. *J. Memb. Sci.* **2011**, *378*, 28–34. [CrossRef]

22. Fernandez, E.; Medrano, J.A.; Melendez, J.; Parco, M.; Viviente, J.L.; van Sint Annaland, M.; Pacheco Tanaka, D.A. Preparation and characterization of metallic supported thin Pd–Ag membranes for hydrogen separation. *Chem. Eng. J.* **2016**, *305*, 182–190. [CrossRef]

23. Calles, J.A.; Sanz, R.; Alique, D.; Furones, L. Thermal stability and effect of typical water gas shift reactant composition on H_2 permeability through a Pd-YSZ-PSS composite membrane. *Int. J. Hydrogen Energy.* **2014**, *39*, 1398–1409. [CrossRef]

24. Santucci, A.; Borgognoni, F.; Vadrucci, M.; Tosti, S. Testing of dense Pd–Ag tubes: Effect of pressure and membrane thickness on the hydrogen permeability. *J. Memb. Sci.* **2013**, *444*, 378–383. [CrossRef]

25. Tosti, S. Supported and laminated Pd-based metallic membranes. *Int. J. Hydrog. Energy* **2003**, *28*, 1445–1454. [CrossRef]

26. Nayebossadri, S.; Fletcher, S.; Speight, J.D.; Book, D. Hydrogen permeation through porous stainless steel for palladium-based composite porous membranes. *J. Memb. Sci.* **2016**, *515*, 22–28. [CrossRef]

27. Nakajima, T.; Kume, T.; Ikeda, Y.; Shiraki, M.; Kurokawa, H.; Iseki, T.; Kajitani, M.; Tanaka, H.; Hikosaka, H.; Takagi, Y.; et al. Effect of concentration polarization on hydrogen production performance of ceramic-supported Pd membrane module. *Int. J. Hydrog. Energy* **2015**, *40*, 11451–11456. [CrossRef]

28. Abate, S.; Díaz, U.; Prieto, A.; Gentiluomo, S.; Palomino, M.; Perathoner, S.; Corma, A.; Centi, G. Influence of Zeolite Protective Overlayer on the Performances of Pd Thin Film Membrane on Tubular Asymmetric Alumina Supports. *Ind. Eng. Chem. Res.* **2016**, *55*, 4948–4959. [CrossRef]

29. Melendez, J.; Fernandez, E.; Gallucci, F.; van Sint Annaland, M.; Arias, P.L.; Tanaka, D.A.P. Preparation and characterization of ceramic supported ultra-thin (~1 μm) Pd-Ag membranes. *J. Memb. Sci.* **2017**, *528*, 12–23. [CrossRef]

30. Richter, H. 4—Large-scale ceramic support fabrication for palladium membranes. In *Palladium Membrane Technology for Hydrogen Production, Carbon Capture and Other Applications*; Woodhead Publishing: Cambridge, UK, 2015; pp. 69–82. [CrossRef]

31. Huang, Y.; Dittmeyer, R. Preparation of thin palladium membranes on a porous support with rough surface. *J. Memb. Sci.* **2007**, *302*, 160–170. [CrossRef]

32. Lee, J.-H.; Han, J.-Y.; Kim, K.-M.; Ryi, S.-K.; Kim, D.-W. Development of homogeneous Pd–Ag alloy membrane formed on porous stainless steel by multi-layered films and Ag-upfilling heat treatment. *J. Memb. Sci.* **2015**, *492*, 242–248. [CrossRef]

33. Sanz, R.; Calles, J.A.; Alique, D.; Furones, L.; Ordóñez, S.; Marín, P.; Corengia, P.; Fernandez, E. Preparation, testing and modelling of a hydrogen selective Pd/YSZ/SS composite membrane. *Int. J. Hydrog. Energy* **2011**, *36*, 15783–15793. [CrossRef]

34. Zhang, K.; Gao, H.; Rui, Z.; Liu, P.; Li, Y.; Lin, Y.S. High-Temperature Stability of Palladium Membranes on Porous Metal Supports with Different Intermediate Layers. *Ind. Eng. Chem. Res.* **2009**, *48*, 1880–1886. [CrossRef]

35. Zheng, L.; Li, H.; Xu, H. "Defect-free" interlayer with a smooth surface and controlled pore-mouth size for thin and thermally stable Pd composite membranes. *Int. J. Hydrog. Energy* **2016**, *41*, 1002–1009. [CrossRef]

36. Mateos-Pedrero, C.; Soria, M.A.; Rodríguez-Ramos, I.; Guerrero-Ruiz, A. Modifications of porous stainless steel previous to the synthesis of Pd membranes. In *Studies in Surface Science and Catalysis*; Elsevier: Amsterdam, The Netherlands, 2010; pp. 779–783.

37. Yepes, D.; Cornaglia, L.M.; Irusta, S.; Lombardo, E.A. Different oxides used as diffusion barriers in composite hydrogen permeable membranes. *J. Memb. Sci.* **2006**, *274*, 92–101. [CrossRef]

38. Nam, S.-E.; Lee, K.-H. Hydrogen separation by Pd alloy composite membranes: Introduction of diffusion barrier. *J. Memb. Sci.* **2001**, *192*, 177–185. [CrossRef]

39. Calles, J.A.; Sanz, R.; Alique, D. Influence of the type of siliceous material used as intermediate layer in the preparation of hydrogen selective palladium composite membranes over a porous stainless steel support. *Int. J. Hydrog. Energy* **2012**, *37*, 6030–6042. [CrossRef]

40. Qiao, A.; Zhang, K.; Tian, Y.; Xie, L.; Luo, H.; Lin, Y.S.; Li, Y. Hydrogen separation through palladium–copper membranes on porous stainless steel with sol–gel derived ceria as diffusion barrier. *Fuel* **2010**, *89*, 1274–1279. [CrossRef]

41. Tong, J.; Matsumura, Y.; Suda, H.; Haraya, K. Thin and dense Pd/CeO$_2$/MPSS composite membrane for hydrogen separation and steam reforming of methane. *Sep. Purif. Technol.* **2005**, *46*, 1–10. [CrossRef]

42. Ryi, S.-K.; Ahn, H.-S.; Park, J.-S.; Kim, D.-W. Pd-Cu alloy membrane deposited on CeO2 modified porous nickel support for hydrogen separation. *Int. J. Hydrog. Energy* **2014**, *39*, 4698–4703. [CrossRef]

43. Tarditi, A.; Gerboni, C.; Cornaglia, L. PdAu membranes supported on top of vacuum-assisted ZrO2-modified porous stainless steel substrates. *J. Memb. Sci.* **2013**, *428*, 1–10. [CrossRef]

44. Tanaka, D.A.P.; Tanco, M.A.L.; Okazaki, J.; Wakui, Y.; Mizukami, F.; Suzuki, T.M. Preparation of "pore-fill" type Pd–YSZ–γ-Al2O3 composite membrane supported on α-Al2O3 tube for hydrogen separation. *J. Memb. Sci.* **2008**, *320*, 436–441. [CrossRef]

45. Hwang, K.-R.; Oh, D.-K.; Lee, S.-W.; Park, J.-S.; Song, M.-H.; Rhee, W.-H. Porous stainless steel support for hydrogen separation Pd membrane; fabrication by metal injection molding and simple surface modification. *Int. J. Hydrog. Energy* **2017**, *42*, 14583–14592. [CrossRef]

46. Wang, X.; Tan, X.; Meng, B.; Zhang, X.; Liang, Q.; Pan, H.; Liu, S. TS-1 zeolite as an effective diffusion barrier for highly stable Pd membrane supported on macroporous [small alpha]-Al$_2$O$_3$ tube. *RSC Adv.* **2013**, *3*, 4821–4834. [CrossRef]

47. Bosko, M.L.; Ojeda, F.; Lombardo, E.A.; Cornaglia, L.M. NaA zeolite as an effective diffusion barrier in composite Pd/PSS membranes. *J. Memb. Sci.* **2009**, *331*, 57–65. [CrossRef]

48. Nozaki, T.; Hatano, Y.; Yamakawa, E.; Hachikawa, A.; Ichinose, K. Improvement of high temperature stability of Pd coating on Ta by HfN intermediate layer. *Int. J. Hydrog. Energy* **2010**, *35*, 12454–12460. [CrossRef]

49. Samingprai, S.; Tantayanon, S.; Ma, Y.H. Chromium oxide intermetallic diffusion barrier for palladium membrane supported on porous stainless steel. *J. Memb. Sci.* **2010**, *347*, 8–16. [CrossRef]

50. Guazzone, F.; Engwall, E.E.; Ma, Y.H. Effects of surface activity, defects and mass transfer on hydrogen permeance and n-value in composite palladium-porous stainless steel membranes. *Catal. Today* **2006**, *118*, 24–31. [CrossRef]

51. Ma, Y.H.; Akis, B.C.; Ayturk, M.E.; Guazzone, F.; Engwall, E.E.; Mardilovich, I.P. Characterization of Intermetallic Diffusion Barrier and Alloy Formation for Pd/Cu and Pd/Ag Porous Stainless Steel Composite Membranes. *Ind. Eng. Chem. Res.* **2004**, *43*, 2936–2945. [CrossRef]

52. Iulianelli, A.; Alavi, M.; Bagnato, G.; Liguori, S.; Wilcox, J.; Rahimpour, R.M.; Eslamlouyan, R.; Anzelmo, B.; Basile, A. Supported Pd-Au Membrane Reactor for Hydrogen Production: Membrane Preparation, Characterization and Testing. *Molecules* **2016**, *21*, 581. [CrossRef]

53. Sanz, R.; Calles, J.A.; Alique, D.; Furones, L. New synthesis method of Pd membranes over tubular {PSS} supports via "pore-plating" for hydrogen separation processes. *Int. J. Hydrog. Energy* **2012**, *37*, 18476–18485. [CrossRef]

54. Sanz, R.; Calles, J.A.; Ordóñez, S.; Marín, P.; Alique, D.; Furones, L. Modelling and simulation of permeation behaviour on Pd/PSS composite membranes prepared by "pore-plating" method. *J. Memb. Sci.* **2013**, *446*, 410–421. [CrossRef]

55. Mardilovich, I.P.; Engwall, E.; Ma, Y.H. Dependence of hydrogen flux on the pore size and plating surface topology of asymmetric Pd-porous stainless steel membranes. *Desalination* **2002**, *144*, 85–89. [CrossRef]

56. Baker, R.W. *Membrane Technology and Applications*; John Wiley & Sons: Hoboken, NJ, USA, 2004; pp. 301–353. [CrossRef]

57. Han, J.-Y.; Kim, C.-H.; Lim, H.; Lee, K.-Y.; Ryi, S.-K. Diffusion barrier coating using a newly developed blowing coating method for a thermally stable Pd membrane deposited on porous stainless-steel support. *Int. J. Hydrog. Energy* **2017**, *42*, 12310–12319. [CrossRef]

58. Washington, P. *II.C.3 High Performance Palladium-Based Membrane for Hydrogen Separation and Purification*; Department of Energy: Washington, DC, USA, 2011; pp. 58–61.